

Kinetic study of the electroreduction of nitrobenzene

T. R. NOLEN, P. S. FEDKIW*

Department of Chemical Engineering, North Carolina State University, Raleigh, NC 27695-7905, USA

Received 3 May 1989; revised 25 July 1989

A reaction kinetic study has been performed for the reduction of nitrobenzene on a Cu electrode in 1 M H₂SO₄ in a 50 : 50 (Vol %) mixture of water and 1-propanol at 27°C. The study was carried out on a rotating disc electrode for which the current–potential data were supplemented with product–concentration measurements. The resulting rate expressions represent a reaction mechanism for the reduction of nitrobenzene to aniline and p-aminophenol through the common intermediate phenylhydroxylamine, and incorporate the dependence on reactant concentration and potential for the three predominant reaction pathways. The three major reaction steps were studied independently by performing experiments in which phenylhydroxylamine only was used as the reactant to complement those experiments in which nitrobenzene was used. The kinetic expressions found from measuring the rates of the individual reactions were consistent with the results of experiments in which all the reactions were carried out simultaneously. The expressions obtained are suitable for use in reactor design, modelling and control, and of equal importance, the methodology outlined to extract kinetic parameters from the current and concentration data serves as a model for application to other reaction systems.

Nomenclature

A	electrode area (cm ²)
D	diffusion coefficient (cm ² s ⁻¹)
E	electrode potential (V)
F	Faraday's constant, 96485 (C mol ⁻¹)
i_H	current density due to the hydrogen evolution reaction (A cm ⁻²)
I	current (A)
I_k	kinetic current (A)
I_L	limiting current (A)
k_1	rate constant for the reduction of nitrobenzene to phenylhydroxylamine (cm s ⁻¹)
k_2	rate constant for the reduction of phenylhydroxylamine to aniline (cm s ⁻¹)

k_3	rate constant for the rearrangement of phenylhydroxylamine to p-aminophenol (s ⁻¹)
n	number of electrons per equivalent
T	temperature (K)
X	fractional conversion of phenylhydroxylamine to p-aminophenol

Greek

δ_i	diffusion layer thickness of species i (cm)
κ	conductivity (cm ⁻¹ ohm ⁻¹)
μ	viscosity (g cm ⁻¹ s ⁻¹)
ν	kinematic viscosity (cm ² s ⁻¹)
ρ	density (g cm ⁻³)
ω	rotation speed of electrode (s ⁻¹)

1. Introduction

Although numerous studies have been performed on the electrochemical reduction of nitrobenzene, the approach taken in most of this work is from a chemistry point of view in which fundamental reaction processes are identified and *qualitative* descriptions are deduced for the reaction mechanism. In contrast, the methods used in the present work are based on a reaction engineering approach in which concentration data for products obtained from chromatographic analysis are used to supplement the information from the measured currents to deduce rate expressions. Concentration–time data are not often used in electrochemical kinetic studies even though these can serve as a valuable complement to the polarization behaviour. The goal of this work is to obtain *quantitative* rate

expressions for the reduction of nitrobenzene (with identification of only the major reaction pathways) which may consequently be used in reactor design.

Earlier studies [1–3] of the reduction of nitrobenzene suggest that the simplified mechanism, shown in Fig. 1, is applicable on a Cu electrode in a deoxygenated water/alcohol acid solution. In this simplified mechanism, nitrobenzene (NB) is first reduced to phenylhydroxylamine (PHA) which in turn can be electrochemically reduced to aniline (AN) or can rearrange chemically to p-aminophenol (PAP).

Even though the reduction of NB has been studied extensively [3–6], no data were found in the literature that would provide usable rate expressions for this simplified mechanism. Fleischmann *et al.* [6] studied the reduction of NB on Hg electrodes and considered the electrochemistry of major species involved in the

*Author to whom correspondence should be addressed.

reaction sequence. However, strict control of mass transfer was not possible because of the use of a mercury-pool electrode. A recent study by Clark *et al.* [3] reports quantitative rate expressions for the reduction of NB at 55°C for the production of PAP, o- and p-anisidine and AN in a solution of 10 vol % sulphuric acid in methanol. Clark *et al.* used a reaction engineering approach, but their approach differs from the present study in several respects. We have made comprehensive use of the rotating disc electrode (RDE) and its well-known transport properties, using concentration measurements for rate data, determining individual diffusion coefficients for both NB and PHA, and using PHA as a starting material in order to study each reaction sequence separately. Although more effort is required to utilize these analytical methods than is required for the methods used by Clark *et al.*, the resulting rate expressions obtained are thought to be more reflective of the actual reaction kinetics because of the decreased number of assumptions.

It should be emphasized that the purpose of the present study is to deduce quantitative kinetic expressions for a model reaction sequence to use in electrochemical reactor studies. Consequently, although the reaction itself is of commercial interest [7, 8], the conditions for this study were chosen for convenience and suitability for modelling purposes and not for commercial application. The work presented here is a complete account of the preliminary results presented earlier [9].

The reactions in the simplified mechanism for the reduction of NB shown in Fig. 1 are, of course, not elementary steps and, in fact, the detailed mechanism of the elementary steps is more complex [4]. For the purpose of an engineering study, it is not feasible to determine quantitative rate expressions for all the elementary reactions individually; however, every effort was made to establish the validity of the simplification by using an array of different experiments with cross-comparison of the results including:

(a) studying each electrochemical reaction individually in differential-conversion experiments using the current to provide rate information,

(b) studying the homogeneous chemical rearrangement of PHA to PAP in an integral-conversion batch reactor with no electrode present, and

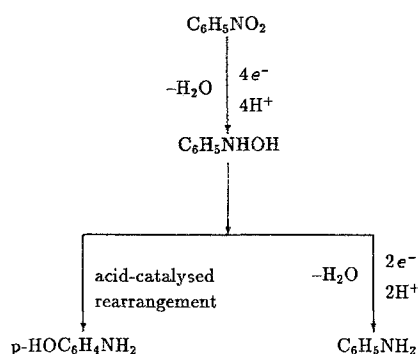


Fig. 1. Simplified mechanism for the reduction of nitrobenzene on a copper electrode in a deoxygenated, acid water/propanol solution [3].

(c) performing integral-conversion experiments at constant potential in which both chemical and electrochemical reactions occur simultaneously and comparing the results to those predicted using the kinetic constants determined from the experiments in which the reactions were studied individually.

2. Experimental details

The electrolyte (1 M H₂SO₄ in 50:50 vol % H₂O:1-propanol) and the electrode material (Cu) were chosen on the basis of earlier studies [1, 2] with a reaction temperature of 27°C chosen for experimental convenience. Since the hydrogen ion concentration in the reactor is essentially constant, the dependence of the reactions on pH was lumped implicitly in the rate constant. A list of the physical parameters determined in this study is given in Table 1.

The working electrode for most experiments consisted of a 5.0 mm diameter Cu rod (99.999%) encased in a 13 mm diameter Teflon sheath so that the end of the rod formed a Cu disc. A catholyte volume of 43 cm³ was used in experiments with this electrode. The Cu working electrode was rotated using an ASR2 rotator from Pine Instrument Company. The Cu surface was prepared for an experiment by mechanical polishing with 0.05 μm Al₂O₃ (Buehler) followed by rinsing twice with DI water in an ultrasonic bath for 10 min. A PAR 173/179 potentiostat/coulometer was used for potential control. In some integral-conversion experiments, a 13.0 mm diameter Cu electrode was used with a catholyte volume of 147 cm³, and the concentrations of reactants and products were determined using an HPLC analysis method. The HPLC analysis was carried out by a method similar to that presented by Sternson and DeWitte [10], and further details can be found in [11].

The uniformity of the current distribution on the RDE was estimated using the method described by Albery and Hitchman [12] which showed that, under the most non-uniform conditions, the current across the disc varied by less than 10% from the average for the 5 mm electrode but by up to 30% for the 13 mm electrode. Even so, the data collected with the 13 mm electrode agreed well with that for the smaller electrode. Correction for the ohmic resistance between the reference and working electrode was made using the primary current distribution resistance [13].

A standard three-electrode electrolysis cell was used with a Nafion membrane to separate the Pt gauze counterelectrode compartment from the catholyte compartment. All potentials reported are relative to

Table 1. Summary of the physical parameters at 27°C

$D_{\text{NB}} = 4.4 \times 10^{-6} \text{ cm}^2 \text{ s}^{-1}$
$D_{\text{PHA}} = 2.1 \times 10^{-6} \text{ cm}^2 \text{ s}^{-1}$
$\mu = 0.0260 \text{ g cm}^{-1} \text{ s}^{-1}$
$\rho = 0.975 \text{ g cm}^{-3}$
$\kappa = 0.110 \text{ cm}^{-1} \text{ ohm}^{-1}$

the saturated calomel electrode (SCE) and ohmically corrected. The anolyte and catholyte were degassed by Ar that had been passed over Cu turnings at 350°C, cooled and saturated with the solvent before introduction into the cell. Prior to addition of the reactant, pre-electrolysis was performed with a large area Cu working electrode by passing 2 mA of current for 2 h.

PHA was prepared by reducing NB with Zn powder as described by Kamm [14] and the crude product was recrystallized twice from benzene using petroleum ether (m.p. 82–83°C). The homogeneous chemical rearrangement of PHA to PAP was studied in a glass vessel with no electrode present using HPLC analysis to determine the concentration of PAP with time.

3. Results and discussion

3.1. Electroreduction of nitrobenzene to phenylhydroxylamine

The diffusion coefficient for NB was measured from the limiting current plateaux at different rotation speeds using $n = 4$ (verified by HPLC measurements) and the Levich equation [15]. As an internal consistency check, the diffusion coefficients were also extracted from the experiments performed below the limiting current from the slope of the $1/I$ against $1/\omega^{1/2}$ curves (Equation 1). The diffusion coefficient measured by the two methods for NB was $4.4 \times 10^{-6} \text{ cm}^2 \text{ s}^{-1}$ ($\pm 5\%$). Pseudo-first order electrochemical rate constants (k_1) were obtained from current-rotation speed data at a given potential as suggested by Bard and Faulkner [15],

$$\frac{1}{I} = \frac{1}{I_k} + \frac{1}{0.62nFA[\text{NB}]_{\text{bulk}} D^{2/3} \nu^{-1/6} \omega^{1/2}} \quad (1)$$

$$I_k = nFAk(E)[\text{NB}]_{\text{bulk}}^m \quad (2)$$

where I is the total current, I_k is the kinetic current (that is, the current with no mass transfer limitations as written in Equation 2), D is the diffusion coefficient and ν is the kinematic viscosity. The experiments were carried out using different bulk concentrations of NB (25.6–67.5 mM). Plots of I_k against bulk NB concentration show that I_k for the reduction of NB is linear in NB concentration ($m = 1$ in Equation 2). Figure 2 shows that potential dependence of the rate constant k_1 can be represented by a Tafel-type kinetic expression. Current data only were used to calculate the rate constant for the reduction of NB to PHA. Consequently, it was necessary to perform a few experiments to confirm that, at the potentials studied, the current was primarily due to the reduction of NB to PHA. The concentration-time data did indeed confirm this. For example, in an experiment at 1400 r.p.m., -0.5 V (against saturated calomel electrode (SCE)) and $[\text{NB}]_{\text{bulk}} = 50 \text{ mM}$, only 1.4% of the current went to AN production and only 0.33% went to hydrogen production, as estimated by the measurement of the background current with no NB present.

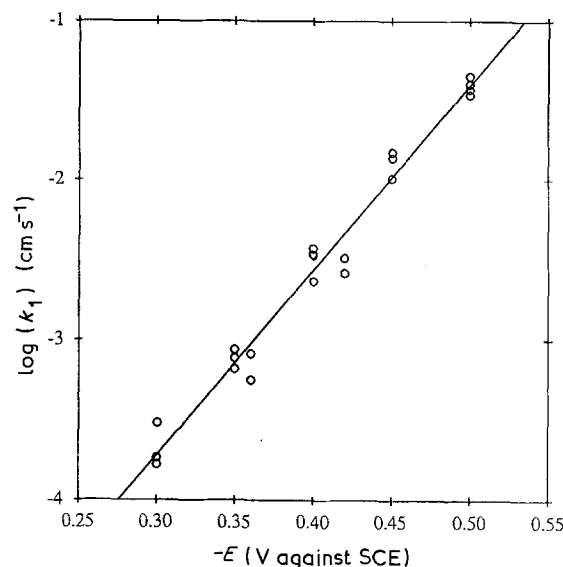


Fig. 2. The potential dependence of the first-order rate constant for the reduction of NB at 27°C. The rate constant was obtained from the intercepts of $1/I$ against $1/\omega^{1/2}$ plots (i.e. I_k) and includes data taken at six different concentrations from 25.6 to 67.5 M. The Tafel slope is $84 \pm 3 \text{ mV decade}^{-1}$; $k_1 = 6.03 \times 10^{-8} \text{ cm s}^{-1} \exp(-0.693 fE)$.

3.2. Chemical rearrangement of PHA to PAP

The reaction of PHA to PAP is called the Bamberger rearrangement and is an acid-catalyzed, homogeneous chemical reaction which was found to be first order in PHA concentration by Sone *et al.* [16] in purely aqueous sulphuric acid solution at 40°C. In the present study, the reaction was also found to be first order in PHA concentration since (a) plots of $\ln(1 - X)$ against time were linear where X is the fractional conversion of the PHA [17], and (b) the fractional conversion of the PHA with time did not depend on the initial concentration. The first order rate constants (k_3) were determined at temperatures ranging from 30°C to 61°C. Figure 3 is the Arrhenius plot constructed from these data and the activation energy is 100 kJ mol^{-1} . The rate constant at 27°C, the temperature used in the rest of the study, was determined by extrapolation to be $4.77 \times 10^{-6} \text{ s}^{-1}$. The rate constant at 40°C was determined by Sone *et al.* [16] at a pH of 0 to be $1.0 \times 10^{-4} \text{ s}^{-1}$. The value determined at 40°C from Fig. 3 is $0.28 \times 10^{-4} \text{ s}^{-1}$. The difference between the two values is attributable to the presence of the 1-propanol in the solution in the present study which decreases the H^+ concentration and therefore reduces the rate of this acid-catalysed reaction.

3.3. Electroreduction of PHA to AN

The electrochemical reduction of PHA to AN was studied using the in-house synthesized PHA as the reactant. Because the homogeneous chemical rearrangement of PHA to PAP is slow at 27°C, the PHA to AN reaction can be isolated by performing a differential-conversion experiment. (In one hour, which is a typical time required for an experiment,

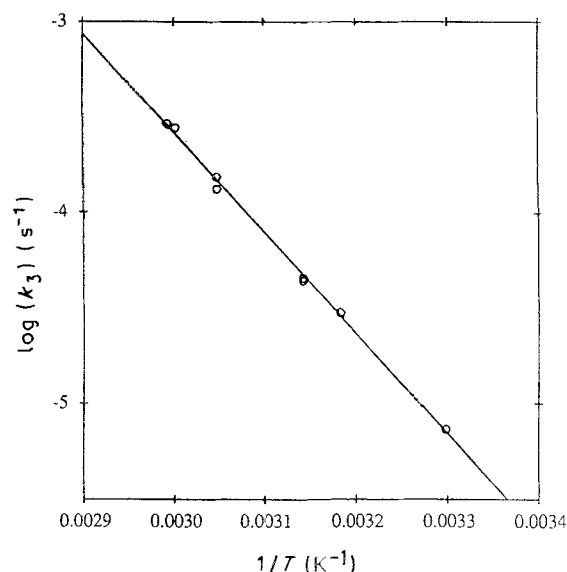


Fig. 3. Arrhenius plot for the first-order rate constant of the Bamberger rearrangement reaction of PHA to PAP in 1 M H_2SO_4 in 50:50 (vol.%) water:1-propanol. Activation energy = 100 kJ mol^{-1} .

only 1.7% of the PHA will react to form PAP.) However, the rate constant for the electroreduction of PHA to AN (k_2) is small enough so that the hydrogen evolution current contributed significantly to the total current. As a means of accounting for this secondary reaction, currents due to hydrogen evolution were measured immediately before introducing PHA into the reactor. In a given experiment, the hydrogen evolution current was subtracted from the current measured after the PHA was added. The hydrogen evolution current was less than 10% of the total in some experiments to as much as 50% in other experiments. Consequently, there is some uncertainty in the differential-conversion experiments for PHA reduction because the rate of hydrogen evolution might be affected by the presence of PHA.

The limiting current for PHA reduction could not be measured because of the hydrogen evolution reaction. Consequently, the limiting current for the two-electron oxidation of PHA to nitrosobenzene in the same solvent on a platinum RDE was used to determine the PHA diffusion coefficient. PHA and nitrosobenzene form a redox couple [4, 18] around +0.35 V against SCE in the electrolyte used in the present study. The identity of the PHA oxidation reaction was confirmed using cyclic voltammetry on solutions containing nitrosobenzene and on solutions containing the in-house synthesized PHA, and in both cases the expected redox couple was observed. The oxidation limiting current experiments showed the diffusion coefficient for PHA to be $2.1 \times 10^{-6} \text{ cm}^2 \text{ s}^{-1}$ ($\pm 10\%$). The values for the diffusion coefficient extracted from the slope of the $1/I$ against $1/\omega^{1/2}$ curves for the reduction of PHA to AN, carried out on the RDE below the limiting current, ranged from 0.7×10^{-6} to $3.9 \times 10^{-6} \text{ cm}^2 \text{ s}^{-1}$. The lack of precision of the differential-conversion experiments in determining the diffusion coefficient is a consequence of the near kinetic-controlled conditions used in these

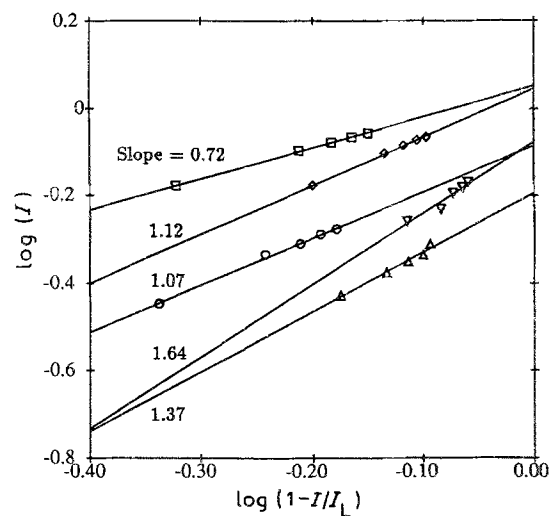


Fig. 4. Plot suggested by Equation 3 to determine the reaction order of the PHA to AN electroreduction. All data shown are for $E = -0.6 \text{ V}$ against SCE. The slopes of these curves (which indicate the reaction order) range from 0.72 to 1.64. There is no trend in the slopes with bulk concentration. I is in mA, $A = 0.196 \text{ cm}^2$. \circ 17.0 mM, \square 32.5 mM, \triangle 35.5 mM, \diamond 46.4 mM, ∇ 74.8 mM.

experiments (because the rate constant is small) resulting in small slopes whose values are susceptible to relatively large experimental error.

The order (m) of the PHA electroreduction reaction was determined from the slope of the $\log(I)$ against $\log(1 - I/I_L)$ plot suggested by the relationship [19]

$$\log I = m \log(1 - I/I_L) + \log I_k \quad (3)$$

where I_L is the calculated limiting current [15]. Figure 4 shows such a plot for $[\text{PHA}]_{\text{bulk}}$ ranging from 17.0 to 74.8 mM. Even though the slopes range from 0.72 to 1.64, no trend is seen with bulk PHA concentration. Also, the data which deviates the most from unity, corresponding to a bulk PHA concentration of 74.8 mM, cover a limited range of $\log(1 - I/I_L)$ and

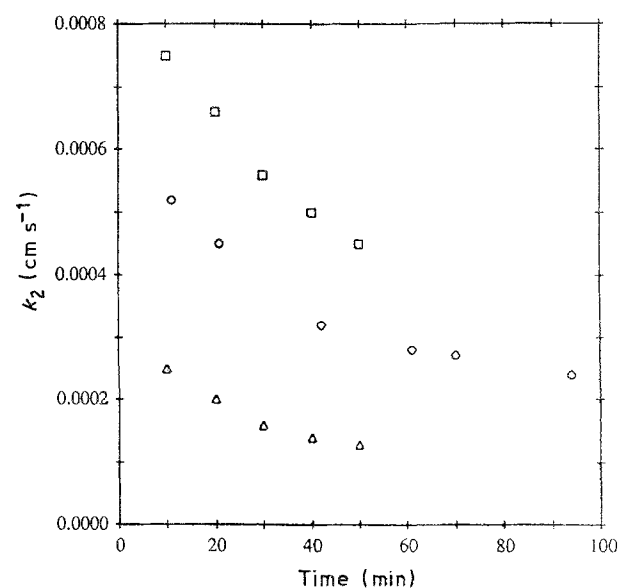


Fig. 5. The first-order rate constant for PHA electroreduction as a function of the time that the electrode is exposed to PHA: \triangle $E = -0.55 \text{ V}$; \circ $E = -0.60 \text{ V}$; and \square $E = -0.65 \text{ V}$ (potential against the SCE).

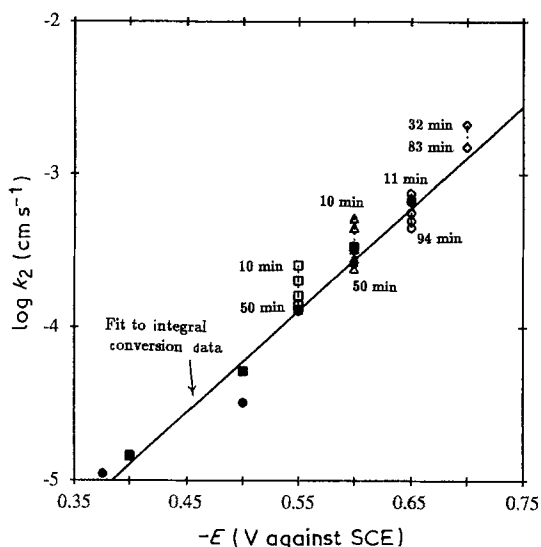


Fig. 6. The first-order rate constant for PHA electroreduction: (a) as a function of time from differential-conversion experiments (open symbols), and (b) from a fit of the integral-conversion RDE model (Table 2) to the integral-conversion experimental data. ■ 13 mm electrode, 1400 r.p.m., $V = 147 \text{ cm}^3$; ● 5 mm electrode, 800 r.p.m., $V = 43 \text{ cm}^3$. The Tafel slope is $150 \pm 12 \text{ mV decade}^{-1}$.

therefore the slope determined from these data is subject to the most uncertainty. We conclude that the apparent reaction order, within reasonable experimental error, is unity over the concentration range studied.

The rate constant for PHA reduction (k_2) was determined as a function of the time the electrode was exposed to PHA in a differential-conversion experiment. Figure 5 shows the apparent first-order rate constant as a function of time as determined from the intercept of plots of $1/I$ against $1/\omega^{1/2}$. The apparent rate constant decreases but seems to asymptote to a constant value at long times. Figure 6 is a plot of the log of the rate constant for PHA reduction against potential and shows both the rate constants determined from integral-conversion experiments, which are discussed later, as well as the rate constants obtained from the differential-conversion experiments as a function of time. The rate constants from the differential-conversion experiments at long times are consistent with the values from the integral-conversion experiments which were carried out over 2 to 4 h.

The change of k_2 with time raises the question of whether the order of the PHA reduction reaction changes with time. The data of Fig. 4 were taken at various times after exposure of the electrode to PHA and no trend in reaction order with time was seen. Also, the agreement between the results of differential- and integral-conversion experiments, which are fundamentally different (as discussed later), suggests that a first-order rate equation for PHA reduction is appropriate for the kinetic model.

3.4. Hydrogen evolution reaction

A rate equation was determined for the hydrogen evolution reaction since it is normally of interest in reactor design. Figure 7 shows the potential dependence

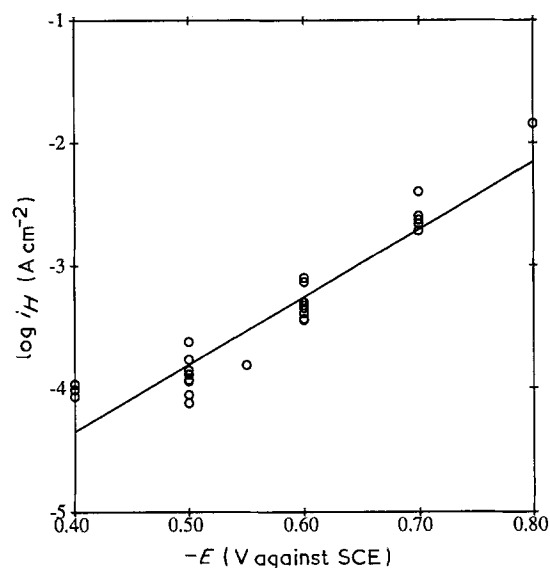


Fig. 7. Potential dependence of the hydrogen evolution current. The Tafel slope is $182 \pm 13 \text{ mV decade}^{-1}$.

dence of the hydrogen evolution current obtained from current measurements taken before PHA was introduced to the reactor for the differential-conversion experiments.

3.5. Integral-conversion experiments

The use of a simplified mechanism involving non-elementary reactions to model the much more complex combination of elementary steps which actually occur clearly requires validation to support the approach. Integral-conversion experiments (that is, those involving conversions of NB of 5–15%) were performed in which all the reactions in the mechanism were occurring simultaneously, as opposed to the differential-conversion experiments in which each major reaction was carried out essentially independently of the others. Another difference between the differential- and integral-conversion experiments is that the latter spanned a longer time. Constant potential and rotation speed were used in these integral-conversion runs.

Figure 8 illustrates the features of a mathematical

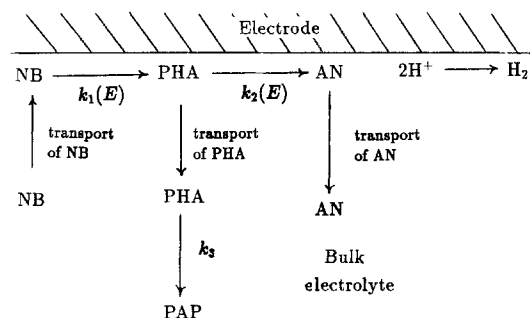


Fig. 8. Schematic of the mass-transfer and reaction processes occurring during the reduction of NB at the rotating disc electrode. NB is transported to the electrode surface where it reacts electrochemically to form PHA which may be reduced to AN, or it may be transported to the bulk electrolyte where it reacts to form PAP. Simultaneously, the hydrogen evolution reaction occurs under kinetic control since the acid is at a high concentration.

model developed to extract kinetic information from the integral-conversion experiments at constant potential and rotation speed and is explained in detail below. The two electrochemical reactants, NB and PHA, are transported to the electrode across two independent diffusion layers. The thickness of the equivalent diffusion layers for the RDE are given by the following equation [15]:

$$\delta_i = 1.61D_i^{1/3}\omega^{-1/2}\nu^{1/6} \quad (4)$$

At the electrode, the three electrochemical reactions shown in Fig. 8 may occur. Some of the PHA produced at the electrode is reduced further to AN while the rest of the PHA is transported to the bulk solution where it may form PAP. The model assumes electrical migration effects are unimportant, the diffusion of NB and PHA are independent of one another, no competitive adsorption occurs on the electrode, no reaction of PHA to PAP occurs in the boundary layer, and the adsorption isotherm is linear and can be incorporated into the first-order rate constant. These assumptions imply a dilute solution in which the diffusion coefficients are constant and only a small fraction of the electrode surface is covered with electroactive species.

Given the physical description provided by Fig. 8, the analytical expressions, shown in Table 2, for the

Table 2. Expressions for the time dependency of the bulk concentrations for the species in an RDE integral-conversion experiment at constant potential and rotation speed. A and V are the electrode area and electrolyte volume, respectively. $[NB]_i$ is the initial bulk concentration of NB. Because the reactions are assumed to be independent of one another, it is not necessary to know the H_2 evolution kinetics to predict the concentrations of the other species

$$[NB] = [NB]_i e^{-k_0 t}$$

$$[PHA] = [NB]_i \frac{k_0'}{k_2'' - k_0'} [e^{-k_0' t} - e^{-k_2'' t}]$$

$$[PAP] = [NB]_i \frac{k_1 k_0'}{k_2'' k_0'} \left[1 + \frac{k_0'}{k_2'' - k_0'} e^{-k_2'' t} - \frac{k_2''}{k_2'' - k_0'} e^{-k_0' t} \right]$$

$$[AN] = [NB]_i \frac{k_3 k_0'}{k_2'' - k_0'} \left[\frac{1}{k_2''} e^{-k_2'' t} - \frac{1}{k_0'} e^{-k_0' t} + \frac{1}{k_0'} - \frac{1}{k_2''} \right] + [NB]_i \frac{k_3'}{k_0'} [1 - e^{-k_0' t}]$$

where

$$k_0' = \frac{A}{V} \left[\frac{k_1}{1 + k_1/m_1} \right]$$

$$k_0'' = k_0' - \frac{k_0' k_2}{k_2 + m_2}$$

$$k_2'' = \frac{A}{V} \frac{m_2 k_2}{k_2 + m_2} + k_3$$

$$k_3' = \frac{k_2 k_0'}{k_2 + m_2}$$

$$k_3'' = \frac{A}{V} \frac{k_2 m_2}{k_2 + m_2}$$

$$m_j = D_j/\delta_j = 0.62D_j^{2/3}\omega^{1/2}\nu^{-1/6}$$

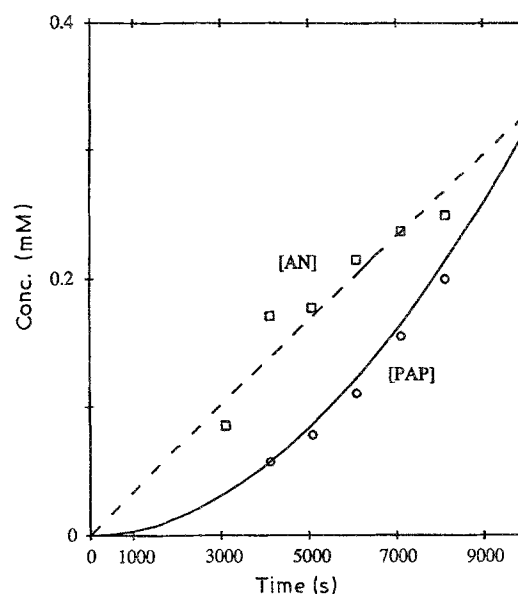


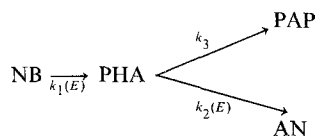
Fig. 9. Calculated (curves) and actual (symbols) concentration-time behaviour for PAP and AN during an integral-conversion experiment. The rate constant for PHA electroreduction to AN was used as an adjustable parameter in the model to fit the experimental data. The electrode rotation speed was 1400 r.p.m. and the potential was -0.5 V against SCE.

changes in bulk concentrations are found by solving the transient material-conservation equations. Since the rate constant for PHA reduction (k_2) decreases significantly with time at the beginning of an experiment, k_2 was used as the only adjustable parameter to fit the experimental AN concentration-time data from the integral-conversion experiments. The value of k_2 so determined is then compared to the value from the differential-conversion experiments, as shown in Fig. 6.

The results extracted from integral-conversion experiments in which NB was used as the starting material using the equations of Table 2 agree with those of the differential-conversion experiments in which PHA was used as the starting material. Obviously, at long times, the 'differential-conversion' experiments involve conversions that can be as high as the integral-conversion experiments. The important point is that the differential- and integral-conversion experiments are fundamentally different; in the differential-conversion experiments, PHA was used as the starting material and rate data were obtained only from the current, corrected for H_2 evolution, while in the integral-conversion experiments, NB was used as the reactant and actual bulk concentration-time data were measured. The agreement between these very different sets of experiments supports the validity of our approach.

Figure 9 shows the results of one typical batch experiment and the best-fit AN simulation results. The predicted and actual PAP concentrations agree fairly well which supports the kinetic expressions obtained for both the reduction of NB to PHA and the chemical rearrangement of PHA to PAP. Other integral-conversion experiments showed equally good agreement between the predicted and measured PAP concentrations and are reported in more detail in [11].

Table 3. Summary of the kinetic parameters determined in this study



$$k_1 = (6.03 \times 10^{-8} \text{ cm s}^{-1}) \exp(-0.693fE)$$

$$k_2 = (2.71 \times 10^{-8} \text{ cm s}^{-1}) \exp(-0.398fE)$$

$$k_3 = 4.77 \times 10^{-6} \text{ s}^{-1}$$

$$i_H = (2.81 \times 10^{-7} \text{ A cm}^{-2}) \exp(-0.328fE)$$

$$T = 300 \text{ K}$$

$$f = F/RT = 38.66 \text{ V}^{-1}$$

$$E = V \text{ against SCE}$$

4. Summary

Engineering kinetic expressions were obtained for a simplified mechanism for the electroreduction of NB on Cu in a deoxygenated acid solution of water and 1-propanol. These expressions are summarized in Table 3 and values of physical parameters determined in this study are given in Table 1. The kinetic expressions reflect the electrode activity that prevails during prolonged electrolysis and, consequently, are most suitable for experiments lasting an hour or more. Various experimental procedures were used in an attempt to establish the validity of the approach used here to obtain these quantitative rate expressions. The complexity of many electroorganic reaction sequences necessitates some simplifications, but blind empiricism is not necessary. The state of electrochemical engineering is today sufficiently advanced to bridge the gap between the complexities of fundamental electrochemistry and the practical design needs of the chemical industry.

Acknowledgement

This work was supported by the National Science Foundation grant CPE 8414166.

References

- [1] P. S. Fedkiw and J. C. Chao, *AIChE J.* **31** (1985) 1578.
- [2] J. Marquez and D. Pletcher, *J. Appl. Electrochem.* **10** (1980) 567.
- [3] J. M. T. Clark, F. Goodridge and R. E. Plimley, *ibid.* **18** (1988) 899.
- [4] H. Lund, in 'Organic Electrochemistry', 2nd ed. (edited by M. Baizer and H. Lund) Marcel Dekker, New York (1983) p. 296.
- [5] S. Swann Jr and R. Alkire, 'Bibliography of Electroorganic Synthesis 1801-1975', Port City Press, Inc., Baltimore, MD (1980).
- [6] M. Fleischmann, I. N. Petrov and W. F. K. Wynne-Jones, 'Proceedings of the First Australian Conference on Electrochemistry', Pergamon Press New York, (1965), p. 500.
- [7] H. V. K. Udupa, *Stud. Org. Chem.* **30** (1987) 457.
- [8] *Idem*, *Indian Chem. Eng.* **30** (1988) 53.
- [9] T. R. Nolen, *J. Electrochem. Soc.* **135** (1988) 29C.
- [10] L. A. Sternson and W. J. DeWitte, *J. Chromatogr.* **137** (1977) 305.
- [11] T. R. Nolen, PhD dissertation, North Carolina State University, Raleigh, NC (1989).
- [12] W. J. Albery and M. L. Hitchman, 'Ring-Disc Electrodes', Clarendon Press, Oxford (1971), Ch. 4.
- [13] J. Newman, *J. Electrochem. Soc.* **113** (1966) 501.
- [14] O. Kamm, 'Organic Synthesis', Vol. 1, John Wiley and Sons, New York, (1948) p. 445.
- [15] A. J. Bard and L. R. Faulkner, 'Electrochemical Methods', John Wiley and Sons, New York, (1980).
- [16] T. Sone, Y. Yokuda, R. Sakai, S. Shinkai and O. Manabe, *J. Chem. Soc., Perkin Trans. 2* **1981(2)** (1981) 298.
- [17] O. Levenspiel, 'Chemical Reaction Engineering', 2nd ed., John Wiley and Sons, New York (1972).
- [18] I. Rubinstein, *J. Electroanal. Chem.* **183** (1985) 379.
- [19] V. Vesovic, N. Anastasijevic and R. R. Adzic, *J. Electroanal. Chem.* **218** (1987) 53.